View metadata, citation and similar papers at core.ac.uk

brought to you by CORE

provided by Open Archive Toulouse Archive Ouverte

Open Archive Toulouse Archive Ouverte (OATAO)

OATAO is an open access repository that collects the work of some Toulouse researchers and makes it freely available over the web where possible.

This is an author's version published in: http://oatao.univ-toulouse.fr/23146

Official URL: http://toc.proceedings.com/40393webtoc.pdf

To cite this version:

Libot, Jean-Baptiste and Alexis, Joël and Arnaud, Lionel and Dalverny, Olivier and Milesi, Philippe and Dulondel, Frédéric Experimental strain energy density dissipated in SAC305 solder joints during different thermal cycling conditions using strain gages measurements. (2018) In: IEEE 68th Electronic Components and Technology Conference, 29 May 2018 - 1 June 2018 (San Diego, United States).

Any correspondence concerning this service should be sent to the repository administrator:

tech-oatao@listes-diff.inp-toulouse.fr

Experimental strain energy density dissipated in SAC305 solder joints during different thermal cycling conditions using strain gages measurements

J-B. Libot, F. Dulondel, P. Milesi
Safran Electronics & Defense
Eragny-sur-Oise, France
jean-baptiste.libot@safrangroup.com,
frederic.dulondel@safrangroup.com,
philippe.milesi@safrangroup.com

J. Alexis, L. Arnaud, O. Dalverny
INP/ENIT LGP
University of Toulouse
Toulouse, France
joel.alexis@enit.fr, lionel.arnaud@enit.fr,
olivier.dalverny@enit.fr

Abstract— **Despite being widely investigated for the last two decades, solder joints thermomechanical durability assessment remains a major concern for industries wishing to switch from lead-based (SnPb) to lead-free electronics. Amongst the variety of lead-free solder compositions, 96.5Sn-3.0Ag-0.5Cu (SAC305) solder alloy has become the preferred substitute to classic SnPb solders. However, unlike SnPb assemblies, the return on experience is limited and the microstructure is very different for SAC305 solder joints. The use of SAC305 solder paste requires to understand the mechanical and fatigue behaviors of the soldered interconnects. This paper presents the experimentation based on strain gages measurements, allowing the determination of the shear stress-strain response of SAC305 solder joints subjected to different thermal cycling conditions. The area of the experimental shear strain-stress hysteresis loops gives the values of the strain energy density corresponding to each thermomechanical loading. The finite element modeling of the test assembly showed a good correlation between experimental and numerical strain energy densities. The experimental shear strain-stress curves also provide the necessary data to derive SAC305 solder joints constitutive laws.**

Keywords- Lead-free, hysteresis, thermal cycling, fatigue, microstructure.

I. INTRODUCTION

Solder joint fatigue is a main reliability concern for aerospace and military industries whose electronic equipment used in the field is required to remain functional under harsh loadings. Electronic assemblies can indeed encounter a wide range of environmental stresses mainly due to thermomechanical loadings eventually leading to temperature-induced solder joints cracking [1]. Due to the RoHS directive which eventually will prevent lead from being utilized in electronic systems, there is a need for a better understanding of lead-free thermomechanical behavior when subjected to temperature variations.

Characterizing solder joints properties remains a challenge as viscoplastic behavior during thermal cycling is complex and since their small dimensions prevent direct measurements from being performed. Energy-based fatigue models, such as Morrow's law, are nowadays widely considered to describe lead-free solder fatigue [2,3]. The use of strain energy density as the fatigue criterion has indeed the advantage to take into account strain and stress amplitudes generated during thermomechanical loading. Most studies consider an approach based on accelerated testing and finite element modeling (FEM) to calculate the strain energy density [4,5]. However, this approach requires prior knowledge of the solder material constitutive laws. Tensile, creep and/or stress relaxation tests are therefore usually conducted in order to determine the elastic, plastic and viscoplastic models associated with the solder material behavior. These constitutive laws are then implemented in FEM software to allow the calculation of stress and strain in solder joints. This methodology nevertheless lacks accuracy as monotonous testing decouples viscoplastic phenomena from each other while they occur simultaneously during thermal cycling. Another way to assess the strain energy density and capture continuous viscoplastic effects during thermal cycles is the construction of the experimental solder joints shear stress-strain hysteresis curve (since this curve is closed, the term "hysteresis loop" will also be used in the rest of the text). This method consists in measuring strains on a strain gages-instrumented test vehicle (four strain gages placed at the center of top and bottom faces of the component and the PCB) during temperature cycles. Based on relevant mechanical hypothesis, the shear strain-stress response of critical solder joints can be determined from the strain measurements. The area of the hysteresis loop gives a measure of the strain energy density dissipated during thermal cycling.

This experimentation has been imagined by P. Hall in 1984 to assess the shear stress and strain in Sn60Pb40 solder interconnects from an 84 I/O Leadless Ceramic Chip Carrier assembly subjected to temperature cycling [6]. P. Hall made the assumption of an axisymmetric model to describe his test vehicle and assess the force and displacement exerted on the critical solder joints (for a peripheral package with no die, the critical solder joints under thermal cycling are localized at the corners of the component: maximum distance between solder joint and neutral axis). Using strain gages adequately placed, P. Hall was able to assess the shear strain and stress in the critical solder joints as functions of the deformations measured with the strain gages. By cross-plotting the temporal evolutions of shear stress and strain, the corresponding Sn60Pb40 hysteresis loop could be plotted. The obtained thermomechanical response was later used by

J-P. Clech to derive Sn60Pb40 solder constitutive laws [7]. Based on an energy-based fatigue model, the same author developed an algorithm to predict the durability of a given electronic assembly from the calculation of the corresponding strain energy density dissipated during thermal cycling [8]. The power of the methodology relies on its double interest: the hysteresis loop construction is 1) a characterization test allowing the determination of solder material behavior laws and it is also 2) a mean to assess thermomechanical damage in solder interconnects during thermal cycling. With the large variety of lead-free compositions coming up on the market and the long-time accelerated testing usually required to qualify a product, this experimentation can be very interesting for companies wishing to reduce time-consuming tests and costs.

Although it appears to be a powerful tool, the hysteresis loop experimentation has never been conducted for lead-free solder joints after reflow assembly. This paper presents the adaptation of P. Hall's original work for SAC305 solder interconnects. Custom daisy-chained 76 I/O Ceramic Ball Grid Array (CBGA76) components were designed and assembled on flame retardant (FR-4) multi-layered (8 copper ground planes) PCB. The component and the PCB were optically characterized to measure their corresponding Coefficient of Thermal Expansion (CTE). Four strain gages were specifically placed at the center of the assembly on top and bottom faces of the PCB and the CBGA76 component. Based on Hall's axisymmetric model which aims to measure the primary effects, strain gages measurements are computed to derive shear stress and strain in the critical interconnects located at the corners of the component. As-reflowed solder joints were also investigated with cross-sections and microscope observations to ensure that the resulting microstructure and grain morphology are representative of those usually observed in SAC305 solder joints after reflow (β-Sn dendrites and Ag_3Sn intermetallic compounds + β-Sn macrograin morphology [9]). The test assemblies were then subjected to four different thermal cycling conditions (three cycles per condition were conducted in order to get the hysteresis loop stabilization):

1) [-25°C, 125°C], 0.5°C/min, 120 minutes dwell,
2) [-40°C, 85°C], 0.5°C/min, 120 minutes dwell,
3) [0°C, 100°C], 0.5°C/min, 120 minutes dwell,
4) [-25°C, 25°C], 0.5°C/min, 120 minutes dwell.

The slow ramp rate (0.5°C/min) and long dwell time allow viscoplastic phenomena (creep and stress relaxation) to occur and prevent any temperature gradient due to differential of thermal inertia between the component and the PCB. The corresponding SAC305 solder joints shear stress-strain hysteresis loops were plotted and the associated strain energy densities were measured. Finite Element Modeling was also conducted in order to compare the experimental and numerical strain energy densities.

II. EXPERIMENTAL APPROACH

A. Principle

P. Hall developed an axisymmetric model to simplify the complex strain field generated in the assembly during temperature cycles. Contrary to classic parallelepipedic packages, the circular model allows the reduction to only one component for the radial force and moment applied on solder joints. This assumption also excludes any out-of-plane forces and only shear solicitations can therefore be considered. This hypothesis is relevant for solder joints subjected to thermal cycling loading. The equivalent axisymmetric model is obtained assuming the same area between the CBGA76 and the circular component: $a^2 = \pi . L_D^2$ (with "a" the side of the CBGA76 and L_D the equivalent radius). Shear displacement and force are indirectly determined with the strain gages which measure strains at the center of top and bottom faces of the component and the PCB. Thermal cycling-induced shear strains in solder joints, which are driven by the CTE mismatch between the component and the PCB, can be divided into two contributions: pure shear and bending of the assembly. Shear stress "τ" can be derived from the forces and moments exerted on the critical solder joints. Figure 1 presents the schematic representation of the test assembly instrumented with four strain gages along with the thermal cycling-induced shear stress and strain at the critical solder joint (to simplify, the assembly bending is not represented in the figure but the term "γ" gathers the pure shear and the bending contributions).

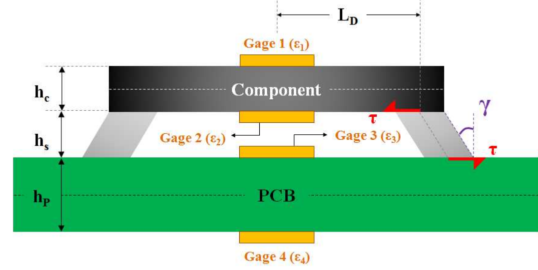

Figure 1. Placement of the four strain gages on the test vehicle (the subscripts "c", "s" and "P" respectively stands for "component", "solder" and "PCB"

From deformations measurements given by the different strain gages and parameters relative to the assembly (dimensions and material properties), shear stress and strain in the critical solder joints can be derived:

Shear strain

$$\gamma = \frac{L_D}{h_s}\left[\varepsilon_3 - \varepsilon_2 + \frac{h_s}{2}\left(\frac{\varepsilon_1 - \varepsilon_2}{h_c} + \frac{\varepsilon_3 - \varepsilon_4}{h_P}\right)\right] \quad (1)$$

Shear stress

$$\tau = \frac{F}{A} = \frac{P\left[\frac{E_c h_c^2(\varepsilon_2 - \varepsilon_1)}{1 - \nu_c} + \frac{2E_P h_P^2(\varepsilon_4 - \varepsilon_3)}{1 - \nu_P^2}\right]}{12\, A\,\left(h_s + \frac{h_c + h_P}{2}\right)} \quad (2)$$

With ε_i the deformation from strain gage "i" (i = 1, 2, 3 and 4), L_D is the equivalent distance to neutral point (radius of the circular component), h is the height, A is the contact area between the solder joint and the component assumed to represent the interfacial crack area generated during thermal cycling), P is the pitch (distance between each solder joint), E is the Young modulus and v is the Poisson ratio.

This section gave a quick overview of the experimentation as imagined and set up by P. Hall in 1984. For more information about this axisymmetric model, the reader can refer to his original paper [6].

B. Test assembly

The test vehicle consists of a custom daisy-chained peripheral 76 I/O Ceramic Ball Grid Array (CBGA76) with 0.76 mm diameter SAC305 solder balls assembled on an FR-4 multi-layered PCB. The component was designed by Kyocera and the balling process was performed by Retronix. The CBGA76 component is a 1 mm thick 25 x 25 mm package with a pitch of 1 mm. Figure 2 shows the CBGA76 package with its associated dimensions.

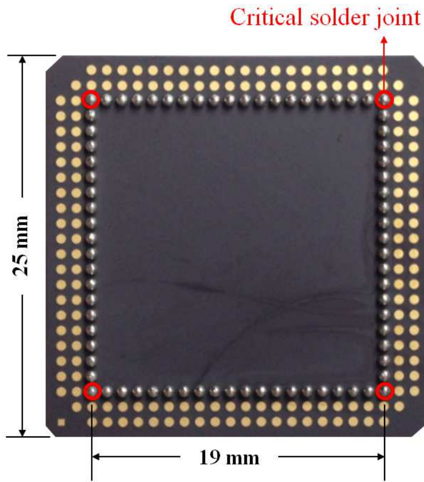

Figure 2. CBGA76 component

Only the inner pads were balled so that there is no "array" effect on strain and stress measured in the critical solder joints. The tungsten, molybdenum (W, Mo) pads are covered with Au, Ni surface finish. The alumina coat on the component bottom face is defined so that the pad opening is equal to 0.6 mm. The size of the inner pads outline is 19 x 19 mm. Based on Hall's assumption stating that the component area should be equal to its corresponding circular plate area, the distance to neutral point (L_D) for the axisymmetric model is 10.7 mm.

The PCB is a 1.6 mm thick, 125 x 125 mm Panasonic R-1755V FR-4 with 8 embedded copper layers. The board has Electroless Nickel Immersion Gold (ENIG) surface finish on Solder Mask Defined (SMD) pads. The conformal coating deposition is defined so that the opening on the PCB pads is equal to 0.6 mm. After reflow, the soldered balls are therefore balanced with the same "solder neck" diameters on the component and PCB sides. The assumed solder crack area is thus $A = \pi \times (0.3)^2 = 0.28$ mm^2. Because of the lack of space between the component and the PCB, Hall was not able to place strain gages 2 and 3 on the same test assembly. To get rid of this limitation, four holes were drilled in the PCB underneath the component (Figure 3). Those holes allow the copper wires from both inside gages (2 and 3) to "go through" the PCB.

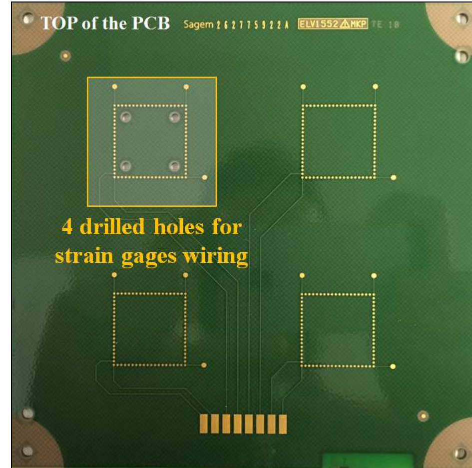

Figure 3. Drilled PCB allowing the placement of the four strain gages on a single test assembly

The PCB and the CBGA76 component were optically characterized with Topography and Deformation Measurements (TDM) in order to determine their respective CTE:

- CBGA76: α_c = 5.5 ppm/°C
- PCB: α_P = 15.4 ppm/°C

During temperature cycling, the dilatations and contractions of the PCB and the CBGA76 component are monitored thanks to four strain gages placed on the assembly with M600 adhesive [10]. Those are rosette gages calibrated with quartz material whose low CTE (α_{quartz} = 0.6 ppm/°C) allows component and PCB thermal strain measurements. Since critical solder joints are located in the diagonals of the CBGA76 component, only the 45°-steered gages are wired. Each strain gage is configured in Wheatstone bridge circuits and wired with 4 wires to ensure accurate resistance measurements (compensation of the resistivity of the wires).

Once the strain gages are placed and wired, the CBGA76 component is deposited on the PCB on which SAC305 solder paste has been first stencil-printed. This pre-assembly is then placed in a reflow oven for final soldering. Figure 4 presents the reflow temperature profile as well as the test vehicle after assembly.

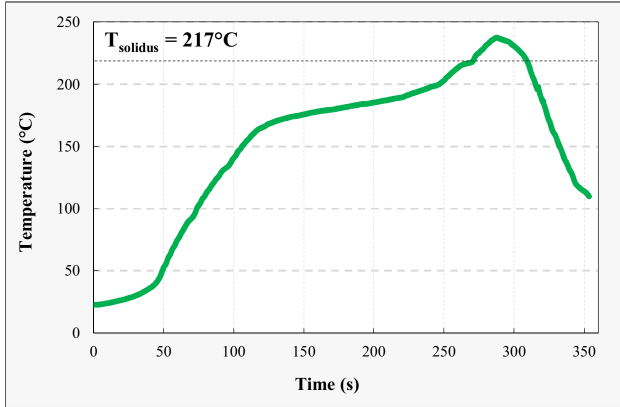

(a)

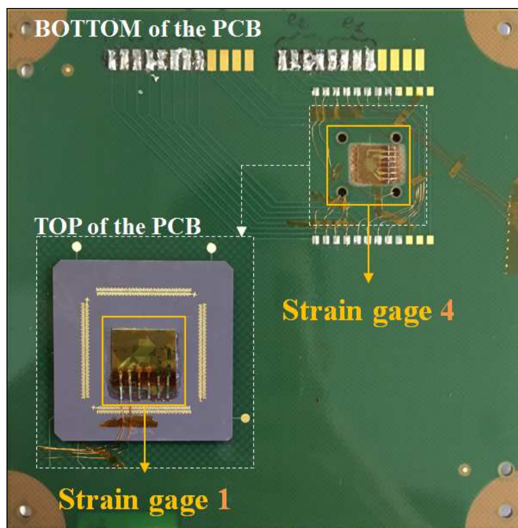

(b)

Figure 4. (a) SAC305 reflow temperature profile. (b) Test assembly after reflow soldering: view of the bottom and top of the PCB with the strain gages 1 and 4 respectively placed on the CBGA76 (TOP) and the PCB (BOTTOM)

The detailed description of the test vehicle and the assembly process is explained in an unpublished paper [11].

C. *As-reflowed solder joints microstructure*

To ensure the representativeness of the experimentation, solder joints microstructure and β-Sn grain morphology after reflow must be similar to those usually observed on SAC305 interconnects. Unlike SnPb solders, SAC305 solder joints are highly anisotropic because of the presence of few large β-Sn macrograins whose Young modulus and CTE vary according to the direction [12]. SAC305 solder joints can also present a localized "interlaced" morphology with smaller β-Sn grains size [9]. It is therefore important to verify whether the CBGA76 solder balls present this specific morphology. Figure 5 (a) presents a cross-section of an as-soldered interconnect under white light and figure 5 (b) shows the same ball under polarized light.

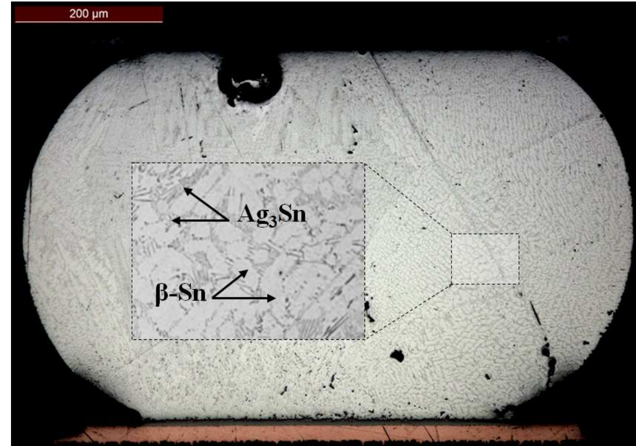

(a)

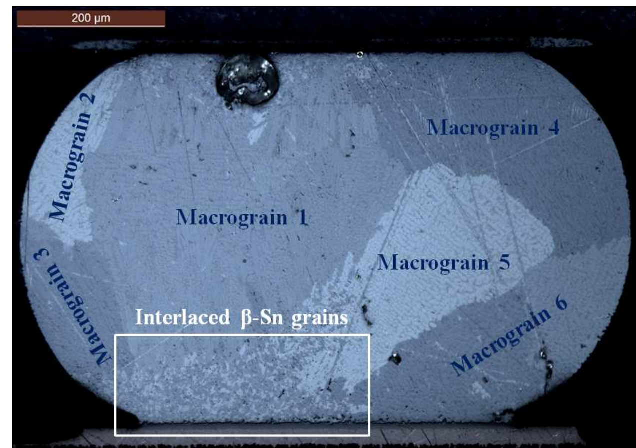

(b)

Figure 5. Observation of a CBGA76 solder ball after reflow under (a) white and (b) polarized light

As expected after solder reflow, SAC305 solder joints depict a β-Sn dendritic microstructure with Ag_3Sn intermetallic compounds and β-Sn matrix filling the inter-dendritic spaces. It is also interesting to observe that SAC305 interconnects exhibit a macrograin morphology along with interlaced grains at the interface with the copper pad.

D. *Temperature cycling tests*

Different thermal cycling conditions are considered in this study. In order to allow viscoplastic phenomena to occur and prevent temperature gradients in the test assembly due to thermal inertia of each material of the CBGA76 component and the PCB, a very slow ramp rate of 0.5°C/min is imposed in the thermal chamber during temperature transitions. Four temperature amplitudes are tested and the dwell time at high and low temperatures is set to 120 minutes. Figure 6 presents the different thermal cycling conditions considered in this study.

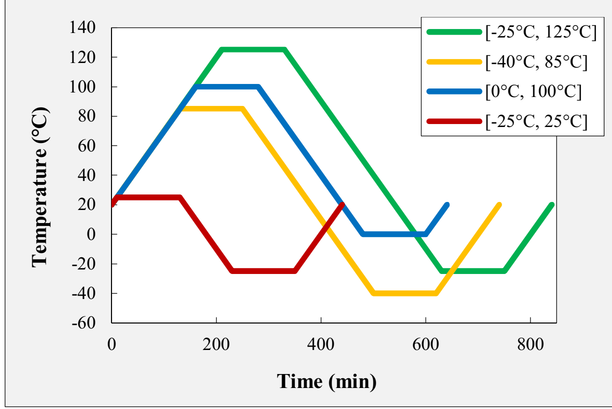

Figure 6. Temperature cycling conditions tested for hysteresis loops construction

III. Finite Element Analysis

The FEM analysis is conducted using ANSYS Workbench V17.1. A slice model of the CBGA76 assembly is considered in this study. This modeling technique applicable to packages having octant symmetry allows the reduction of computing time as it only focuses on the diagonal of the assembly [13]. The assumption is relevant since the outermost corner ball is the most damaged solder joint during thermal cycling. Elastic behavior is considered for the materials of the PCB and CBGA76 component. The elastic properties of each material of the assembly are given in Table 1 below.

TABLE I. Elastic modulus, Poisson ratio and CTE of each material of the test assembly

Material	E (GPa)	ν	CTE (ppm/°C)
FR-4 (PCB)	27.8 (measured)	0.3	15.4 (measured)
Cu	124	0.33	17
Al_2O_3	310	0.27	5.5 (measured)
SAC305	E(T) = -0.14 T(°C) + 35.80 [14]	0.42 [15]	-

The temperature-dependent elastic modulus of SAC305 solder alloy was obtained from tensile tests conducted on dog bone samples at five temperatures from -55°C to 125°C [14]. The β-Sn grain morphology of these samples is not representative of the macrograin morphology usually observed on solder interconnects but it is not problematic here because elastic contribution is not dominant during thermal cycling. SAC305 solder alloy is also described as a viscoplastic material using Anand constitutive model whose parameters are given in Table 2. The viscoplastic contribution is predominant during thermal cycling. The nine Anand constants were therefore determined from creep tests at different temperatures and imposed charges, performed on different dog bone samples depicting a macrograin morphology in order to be consistent with real solder joints after reflow [14].

TABLE II. SAC305 Anand parameters [14]

Parameter	Unit	Value
s_0	MPa	6.0001
Q/R	K	7435.3
A	s^{-1}	3564.7
ξ	-	3.1479
m	-	0.24387
h_0	MPa	20051
$\hat{s}$	MPa	29.652
n	-	0.015665
a	-	2.1314

The strategy to conduct thermomechanical simulation usually consists in calculating the averaged inelastic strain energy density dissipated in the damaged volume of the critical solder joint during one cycle. In this study, another approach is considered as the numerical hysteresis loops are plotted by modeling the strain gages and substituting the calculated strain evolutions into equations (1) and (2).

A fine mesh is attributed to the critical solder joints while a coarser one can be generated for the rest of the assembly to reduce computing time (Figure 7. (a)). Each strain gage is modeled as one shell element with a specific orientation allowing deformation calculations (Figure 7. (b) and (c)).

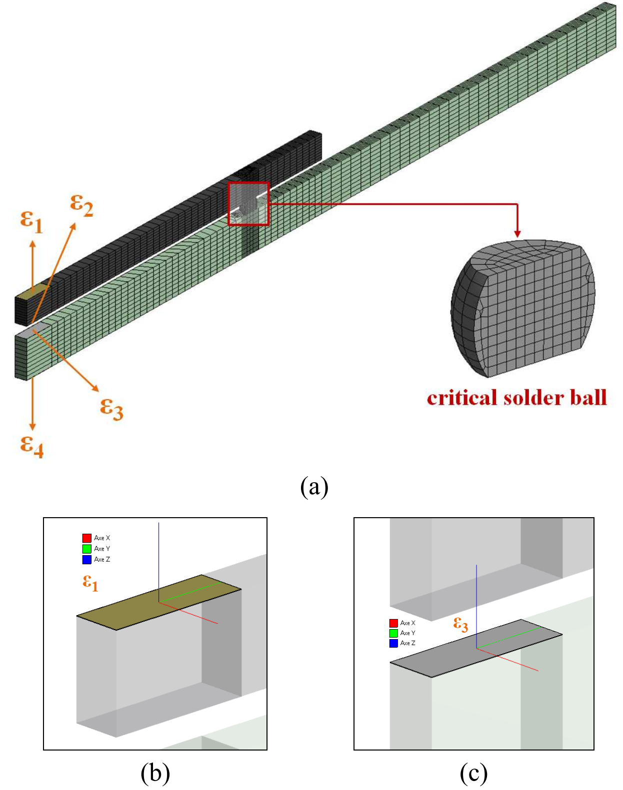

Figure 7. (a) Meshing of the slice model with a focus on the outermost solder ball. Examples of strain gages modeled as shell elements: (b) strain gage 1 and (c) strain gage 3

The numerical model is made of 7224 elements and 36075 nodes (element types: SOLID186, SHELL181, CONTA174 and TARGE170).

IV. Results and Discussion

A. *Experimental SAC305 shear stress-strain hysteresis loop*

Viscoplastic phenomena are believed to occur when $T_H = T/T_m > 0.4$ (T_H is the homologous temperature defined as the ratio between the temperature and the melting temperature of the material T_m) [16]. Between -40°C and 125°C (extrema temperatures for the considered thermal cycling conditions), SAC305 homologous temperatures are respectively close 0.5 and 0.8. In this homologous temperature range, the time-dependent material response, that is to say creep and stress relaxation of SAC305 solder alloy, is significant and thermal cycling-induced viscoplastic effects can therefore be seen from shear stress and strain data collected with strain gages. Figure 8 shows the four shear strain-stress hysteresis loops corresponding to the different temperature cycles. The shape of the hysteresis loops from conditions 1 to 3 is similar. During thermal ramp up, an increase of the shear stress is observed and tends to depict an asymptotic behavior as temperature reaches its maximum value. The high creep rates at high temperature indeed lead to softening of the solder joints. At high temperature dwell, shear stress is released while strain increases. When temperature decreases, the absolute value of shear stress increases but does not show an asymptote as viscoplastic phenomena are less activated at low temperature and solder joints become therefore more resistant. The extent of stress relaxation at low temperature dwell is less important than at high temperature because the creep rates are smaller.

It is interesting to observe that hysteresis curves corresponding to conditions 2 and 3 (yellow and blue loops respectively) seem shifted towards the positive stress values. It is surprising because as temperature increases the interconnections become less resistant to viscoplastic deformations whereas this resistance is higher when temperature decreases. The absolute value of the shear stress should therefore be more important at low temperature than at high temperature. Shizari et al. also observed this trend on solder balls with speckle measurements as they found a value of 15.9 MPa at 105°C and -14.6° MPa at 43°C [17]. However, thermal cycling tests corresponding to these conditions were conducted the following week the test vehicle was reflowed whereas tests corresponding to conditions 1 and 4 were performed several months after reflow assembly. It is believed that during this "isothermal aging" at ambient temperature, the residual stress in solder joints due to assembly flexure generated during assembly was released and that is why the corresponding loops are consistently placed relative to the line $\tau = 0$.

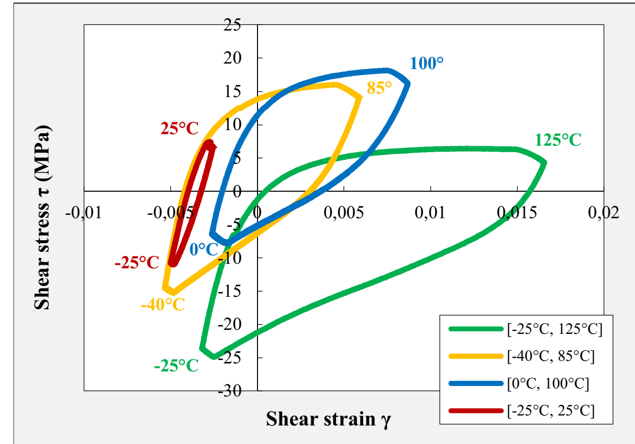

Figure 8. Experimental shear strain-stress hysteresis loops for each thermal cycling condition (the loops were stabilized after 3 cycles)

Temperature cycling conducted between -25°C and 25°C shows a corresponding hysteresis loop with a small area characterizing a limited temperature-induced damage (small dissipated strain energy density). At ambient and low temperatures, viscoplastic contribution (*i.e.* creep and stress relaxation) is indeed not as dominant as at high temperatures. It is therefore expected that CBGA76 assemblies subjected to thermal cycles between -25°C and 25°C would last significantly longer than an assembly subjected to temperature cycling between 25°C and 75°C (same thermal amplitude) for which viscoplastic solicitations are dominant.

B. *Finite Element Modeling analysis*

Numerical simulations of the thermal cycling tests have been performed (Figure 9. (a) and (b)) and a focus has been made on the strain distribution in the solder joints. The obtained strain cartographies are correlated with optical microscopy observations made on cracked CBGA76 solder balls (Figure 10. (a) and (b)). The fatigue crack is located in the solder bulk on the component side. The crack initiates at the solder neck and propagates along the direction parallel to the solder and component interface. The solder neck is a geometrical singularity due to the CBGA76 SMD pads which generates high stress concentration zones from which a crack can initiate.

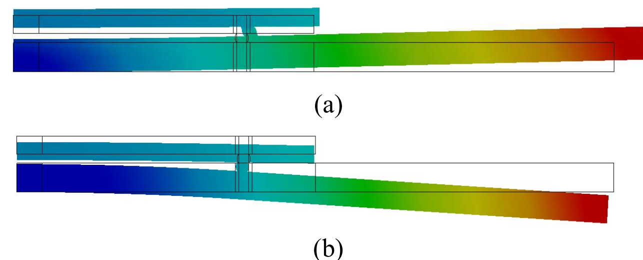

Figure 9. Deformed test assembly at (a) 125°C and (b) -25°C

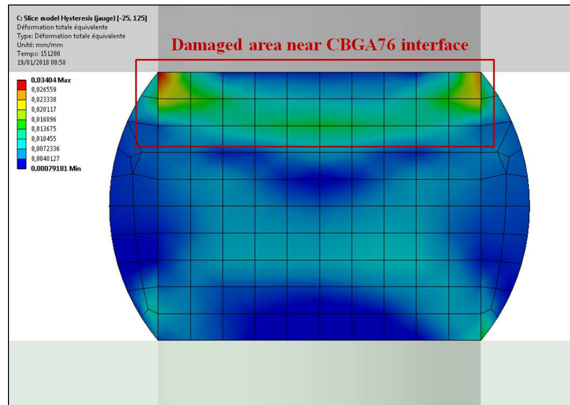

(a)

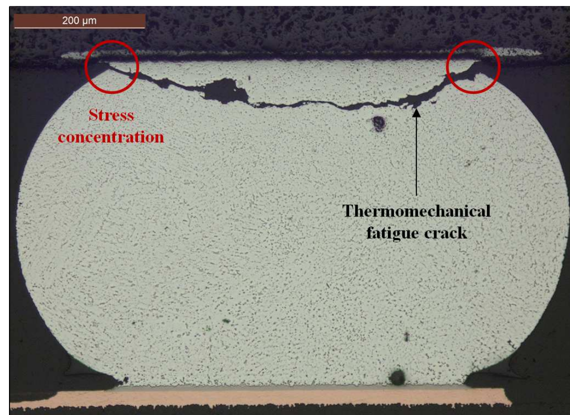

(b)

Figure 10. (a) High strain regions in the critical solder ball determined with FEM analysis. (b) Observation of the thermomechanical fatigue crack localized in the solder bulk on the component side

The FEM analysis qualitatively captures strains in the solder joint. Usually, to assess solder joint durability, the technique consists in calculating the averaged inelastic strain energy in the damaged volume of the critical solder joint. In this analysis, the fatigue criterion is rather calculated by determining the numerical hysteresis loops area. These simulated hysteresis loops are plotted from the deformations obtained from the modeled strain gages. Figure 11 shows the comparison between the experimental and the numerical hysteresis loops for temperature cycling corresponding to conditions 1 between -25°C and 125°C and 4 between -25°C and 25°C (conditions 2 and 3 are not considered for comparison because of the relative position shift which does not allow direct comparison with simulations). For both conditions, the experimental and numerical curves are relatively closed to each other. The discrepancies can be due to the characterization tests considered to derive Anand's parameters. The constitutive viscoplastic model implemented in ANSYS was indeed determined with samples which were not representative of actual solder joints in terms of size and microstructure. On the contrary, the hysteresis loops construction represents a characterization test that considers real size as-reflowed solder joints with a representative microstructure. Moreover, the first set of Anand parameters was determined only from creep tests whereas the current experimentation is conducted with temperature cycling where creep and stress relaxation occur simultaneously as it does for electronic equipment in the field. The experimental hysteresis loops therefore provide the necessary data to improve the accuracy of the viscoplastic model. Coupled with an optimization procedure, the FEM analysis could be used to fit the experimental data and derive new constants of the Anand model.

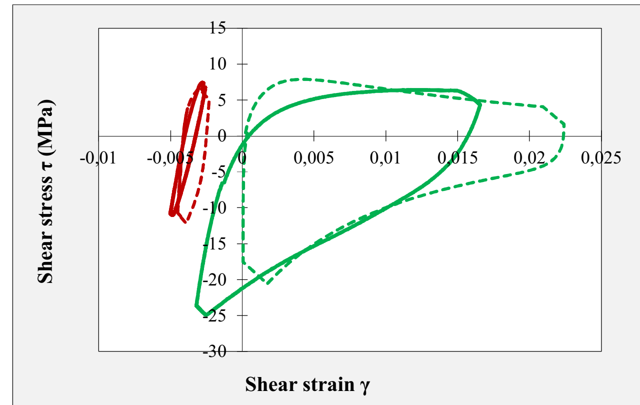

Figure 11. Comparison between experimental (full line) and numerical (dotted line) hysteresis loops for thermal cycling conditions 1 (green loops) and 4 (red loops)

Strain energy densities are measured for each hysteresis loop. The shape of the hysteresis loops, as well as the shear stress and strain ranges are similar between simulation and experimentation for each tested conditions. As a result, the area of the loops, that is to say the experimental and numerical strain energy densities are in a good agreement (Figure 12). The experimental results are particularly interesting as it gives a measured value for a fatigue criterion which is usually determined by calculating the averaged inelastic strain energy density in a specific volume of the solder joints with FEM analysis.

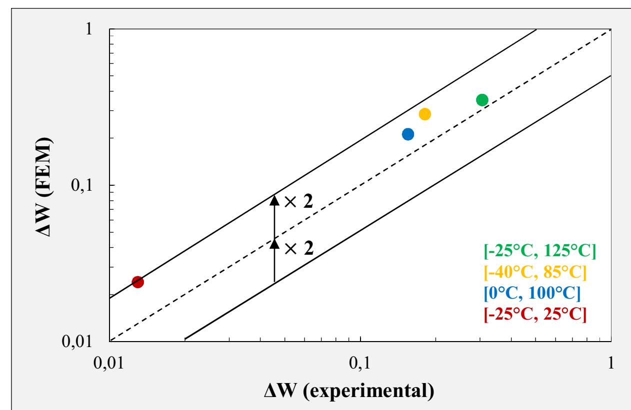

Figure 12. Experimental and numerical strain energy densities for each thermal cycling condition

V. CONCLUSION

A specific test vehicle has been developed to plot experimental shear strain-stress hysteresis loops corresponding to SAC305 thermomechanical behavior. The methodology initially developed by P. Hall in 1984 for Sn60Pb40 solders was apply to assess strain energy densities dissipated in SAC305 solder joints during four thermal cycling tests. FEM analysis was also performed to calculate the numerical strain energy densities which showed a good correlation with the experimentation.

Further work is needed to conduct thermal cycling tests until failure of several test assemblies in order to get a statistical distribution of failures and correlate the associated number of cycles to failure with the measured strain energy density. Conducting such investigation for each thermal cycling condition would allow to derive an entirely experimental fatigue model for SAC305 solder joints subjected to thermomechanical loading.

ACKNOWLEDGMENT

This research work was partially supported by the Federal University of Toulouse Midi-Pyrénées and Safran Electronics & Defense. The author would like to thank N. Caillère, J. Salmon, S. Martin and M-A. Bahi for their help regarding the test vehicles assembly and failure analysis.

REFERENCES

[1] D. Steinberg, “Vibration Analysis for Electronic Equipment”, 3rd edition, John Wiley & Sons, Inc. 2000.

[2] S.K. Sitaraman, K. Kacker, “Chapter 8: Thermomechanical reliability prediction of lead-free solder interconnects", "Lead-Free Solder: Interconnect Reliability”, D. Shangguan, editor, 2005, pp. 181-198.

[3] A. Syed, “Accumulated creep strain and energy density based thermal fatigue life prediction models for SnAgCu solder joints”, Proc. IEEE Symp. Electronic Components and Technology Conference (ECTC 2004), IEEE Press, June 2004, pp. 737-746, doi: 10.1109/ECTC.2004.1319419.

[4] F-X. Che, J-E. Luan, D. Yap, K-Y. Goh, X. Baraton, “Thermal cycling fatigue model development for FBGA assembly with Sn-Ag-based lead-free solder”, Proc. IEEE Symp. International Electronics Manufacturing Technology Conference (IEMT 2008), IEEE Press, Nov. 2008, pp. 1-6, doi: 10.1109/IEMT.2008.5507875.

[5] Tsou, C.Y., Chang, T.N., Wu, K.C., Wu, P.L., Chiang, K.N., “Reliability assessment using modified energy based model for WLCSP solder joints”, Proc. IEEE Symp. International Conference on Electronics Packaging (ICEP 2017), IEEE Press, April 2017, pp. 7-12, doi: 10.23919/ICEP.2017.7939312.

[6] P.M. Hall, “Forces, moments, and displacements during thermal chamber cycling of leadless ceramic chip carriers soldered to printed boards”, IEEE Transactions on Components, Hybrids, and Manufacturing Technology, Vol. CHMT-7, No. 4, Dec. 1984, pp. 314-327.

[7] J-P. Clech, “Solder reliability solutions : a PC-based design-for-reliability tool”, Soldering and Surface Mount Technology, Vol. 9, No. 2, 1997, pp. 45-54.

[8] J-P. Clech, “Chapter 2: Solder properties, joint mechanics, fatigue and failure”, EPSI Inc., 1998-2001.

[9] Arfaei et al., “Improving the thermomechanical behavior of lead free solder joints by controlling the microstructure”, 13th InterSociety Conference on Thermal and Thermomechanical Phenomena in ElectronicSystems, May-June 2012, pp.392-398, doi: 10.1109/ITHERM.2012.6231456.

[10] www.dmesures.fr/images/FT_jauges_accessoires/dtcolles.pdf.

[11] J-B. Libot, J. Alexis, L. Arnaud, O. Dalverny, F. Dulondel, P. Milesi, “Experimental SAC305 shear stress-strain hysteresis loop construction using Hall’s one-dimensional model based on strain gages measurements”, unpublished.

[12] T.R. Bieler, H. Jiang, L. P. Lehman, T. Kirkpatrick and E. J. Cotts, “Influence of Sn Grain Size and Orientation on the Thermomechanical Response and Reliability of Pb-free Solder Joints”, Electronic Components and Technology Conference, May 2008, pp. 1462-1467, doi : 10.1109/TCAPT.2008.916835.

[13] Gustafsson, G., Guven, I., Kradinov, V., Madenci, E., “Finite Element Modeling of BGA packages for life prediction”, Electronic Components and Technology Conference, August 2000, pp. 1059-1063, doi : 10.1109/ECTC.2000.853300.

[14] J-B. Libot, “Fatigue life prediction methodologies of SAC305 assemblies subjected to thermal and vibrational loadings”, PhD dissertation, Federal University of Toulouse Midi-Pyrénées, 2017.

[15] T.T. Nguyen, S. Park, “Characterization of elasto-plastic behavior of actual SAC solder joints for drop test modeling”, Microelectronics Reliability, Vol. 51, 2011, pp. 1385-1392.

[16] Sakai, T., Belakov, A., Kaibshev, R., Miura, H., Jonas, J.J., “Dynamic and post-dynamic recrystallization under hot, cold and severe plastic deformation conditions”, Progress in Materials Science, Vol.60, 2014, pp. 130-207.

[17] A. Shirazi, “A hybrid approach to characterization and life assessment of trilayerassemblies of dissimilar materials under thermal cycles”, PhD dissertation, Ryerson University, 2011.